Phys Chem Minerals (1988) 16:199–206

PHYSICS AND CHEMISTRY OF MINERALS

Simple Covalent Potential Models of Tetrahedral SiO_2: Applications to α-quartz and Coesite at Pressure

Lars Stixrude and M.S.T. Bukowinski
Department of Geology and Geophysics, University of California, Berkeley, CA 94720, USA

Abstract. We present a covalent potential model of tetrahedrally coordinated SiO_2. The interactions include covalent effects in the form of a Si−O bond-stretching potential, O−Si−O and Si−O−Si angle-bending potentials, and oxygen-oxygen repulsion. Calculated equations of state of α-quartz and coesite agree well with experiment (calculated densities within 1 percent of experiment up to 6 GPa). The calculated α-quartz-coesite transition pressure agrees with the experimental value of ≈2 GPa. Furthermore, the compression mechanisms predicted by the model (i.e. pressure induced changes in Si−O bond lengths and O−Si−O and Si−O−Si angles) are accurate.

Introduction

The chemical and thermal state of the Earth through time is controlled largely by the properties of silicates which comprise 83 percent of the planet by volume. Thus, an understanding of the nature of silicates, over the wide range of pressure, temperature and composition encountered in the Earth's interior, is central to geophysics (Bass 1987). The structure and thus all physical properties of silicates vary widely over the mantle's pressure regime (Jeanloz and Thompson 1983). The structural changes, due to compression and phase changes, ultimately depend on the properties of the Si−O bond, the most common chemical bond in the Earth (Gibbs 1982). In order to describe simply the properties of the Si−O bond in silicates and their structural variations, we begin with the compositionally simplest silicate, SiO_2.

SiO_2 like other silicates has distinct low and high pressure structures, the former composed of SiO_4 tetrahedra and the latter of SiO_6 octahedra (the transition occurs at 8 GPa for crystalline SiO_2, Akimoto et al. 1977; 20 GPa for $MgSiO_3$, Liu and Bassett 1986; and may occur gradually above 20 GPa in SiO_2 glass, Williams and Jeanloz 1988). This structural change also involves a change in the electronic properties of Si from sp^3 to sp^3d^2 hybridization. Thus, we do not expect any one model of Si−O bonding to describe both tetrahedral and octahedral phases. Although a model of Si−O bonding must ultimately include octahedral structures as well, we concentrate initially on the tetrahedral structure. Within this framework, we wish to make our model as general as possible, capable of describing the important structural properties of the many crystalline and amorphous forms of tetrahedral SiO_2 as a function of pressure.

To be useful in describing the structure and compression of crystalline and amorphous silica, we believe a model of tetrahedral SiO_2 should meet the following criteria: 1) it must be independent of structural data and yet, 2) it must reproduce the known structure and compressional mechanisms of tetrahedral phases of SiO_2 with reasonable accuracy, 3) it must incorporate the known physics of bonding in SiO_2 at least qualitatively, and 4) it must be as simple as consistency with the available data allows. The first two requirements insure that models can be obtained that are not biased by the structure of a particular phase. This is an important condition, since tetrahedral SiO_2 occurs in at least 9 crystalline polymorphs as well as amorphous and liquid states with large structural differences between them (cf. Liu and Bassett 1982). Thus, it is unlikely that a model specialized to the structure of a particular polymorph will successfully describe the others. The third requirement is obvious. We state it explicitly because it is possible to account for many structural features of SiO_2 polymorphs with purely ionic pair potential models (e.g., Erikson and Hostetler 1987). However, the inadequacy of such models becomes apparent when they are used to compute thermodynamic properties. For example, the computed bulk moduli are invariably much larger than those observed experimentally, as was pointed out by Erikson and Hostetler (1987). The fourth condition allows one to identify which forces are most important for the system or process under study (in our case structure and compression of silicates) and thus which should be included in the model. Adding forces (and parameters) to the model inevitably improves agreement with observation. However, the reason for the improvement may only be the greater flexibility allowed by the additional parameters rather than physical significance of the additional force.

Previous models of SiO_2 do not meet one or more of the criteria described above. Simple ionic models of SiO_2 (Woodcock et al. 1976; Lasaga and Gibbs 1987; Soules 1979; Mitra 1982; Matsui et al. 1982; Hostetler 1982) have been shown to predict bulk moduli of α-quartz and coesite that are too large by as much as an order of magnitude (Erikson and Hostetler 1987; Lasaga and Gibbs 1987). Models that include covalent effects have been reported (e.g. Sanders et al. 1984; Lasaga and Gibbs 1987). The latter authors were able to reproduce the structure of α-quartz at zero pressure but not at higher pressures since their mod-

el predicts a negative K'_0 (pressure derivative of the bulk modulus). Although the former authors produced accurate structural and elastic properties for α-quartz, they used zero pressure structural and elastic properties of α-quartz as constraints. Furthermore, their model includes shell displacements, rendering it too complex for our purposes.

The principal goal of this report is to present a covalent potential model of tetrahedral SiO_2 which satisfies all the above requirements. We first apply the model to α-quartz (hereafter referred to as quartz) and coesite. These minerals were chosen because they are representative of the wide range of structures observed in tetrahedral silica. Quartz is typical of the very open, low pressure structures which are built of predominantly 6-membered rings of tetrahedra, while coesite has the densest crystalline tetrahedral structure, composed of predominantly 4-membered rings. Also, structural and compressional data exist on these minerals which provide an excellent test of our model.

The covalent potential model of SiO_2 is described in detail below. We then discuss the procedure used to constrain the potential parameters. Finally, the properties of quartz and coesite predicted by the model are compared to experimental data: *equations of state* (EOS), the quartz-coesite transition pressure, and compression mechanisms, including changes in Si–O bond length and O–Si–O and Si–O–Si angles.

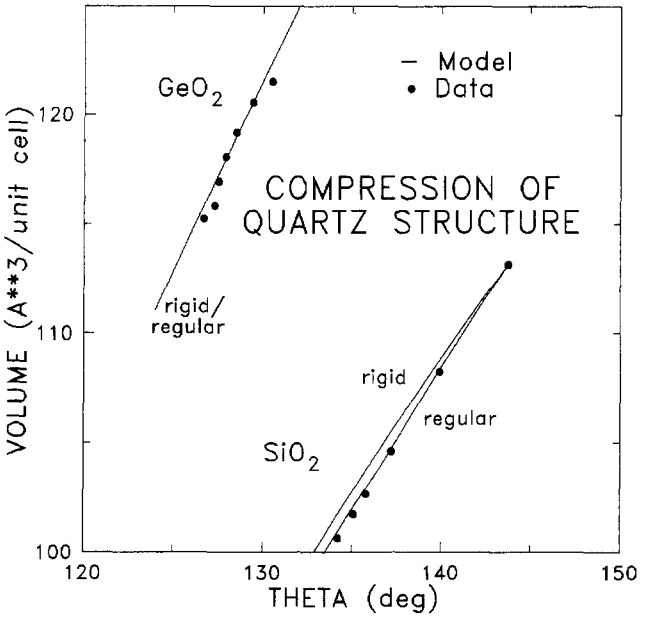

Fig. 1. Volume vs. T–O–T angle for SiO_2 and GeO_2 in the α-quartz structure for regular and rigid tetrahedral models and experiment. Data are from Levien et al. (1980) for SiO_2 and Jorgensen (1978) for GeO_2

The Model

To guide the construction of the model, we first note an important feature of the compression of tetrahedral framework structures: the sharp contrast in compression mechanisms between the nearly rigid tetrahedra and the easily deformable angle subtended by the silicon ions at the oxygens bridging linked tetrahedra (Si–O–Si angle). To show the magnitude of this contrast, we calculate the equation of state for quartz with regular tetrahedra (all O–Si–O angle equal to 109.47°) and for rigid tetrahedra (with the additional constraint that the Si–O bond length remain fixed). Grimm and Dorner (1975) give the formulas necessary to calculate the quartz volume given an Si–O–Si angle and an Si–O bond length. We use the observed volume vs. Si–O bond length dependence of Levien et al. (1980) in the calculations. Figure 1 shows the result of the rigid and regular tetrahedra cases compared to experiment. Within the error of the experiment, the changes in O–Si–O angles with pressure have no effect on the volume of quartz. The rigid tetrahedra case, which differs by no more than 1 percent from experiment, shows the relative unimportance of changes in the Si–O bond length. Also shown in Figure 1 is an analogous comparison for GeO_2 in the quartz structure. Again, the rigid tetrahedral model accounts for the data within the experimental error. Since tetrahedral distortion in low pressure GeO_2 is significantly greater than in high pressure SiO_2 (Jorgensen 1978; Levien et al. 1980), we conclude that changes in Si–O–Si angles are the dominant compression mechanism in tetrahedral phases of SiO_2 throughout their stability field ($P \leq 10$ GPa).

The dichotomy in structural compressibility strongly suggests an analogous dichotomy between intra- and inter-tetrahedral forces. The intra-tetrahedral forces, which keep the tetrahedra rigid, must be strong, while the inter-tetrahedral forces, which accommodate nearly all the compression, must be relatively weak.

More detailed knowledge of the interatomic forces is required to construct the model; for this we turn to the bitetrahedral Si_2O_7 molecule, whose bonding properties have been extensively studied by *Molecular Orbital* (MO) calculations (Gibbs 1982). We assume that bonding in the Si_2O_7 bitetrahedron is similar to bonding in SiO_2 framework structures. This assumption is supported by three observations: 1) the bitetrahedron is the largest unit which they all share; 2) bonding in SiO_2 is largely covalent and thus short range, suggesting that most of the relevant bonding properties are contained in the bitetrahedron and 3) MO calculations show that the bitetrahedron can account for structural systematics in silicates (Gibbs 1982).

We divide the potentials that make up the model into three types: 1) intra-tetrahedral covalent forces, 2) inter-tetrahedral covalent forces and 3) other forces, including O–O repulsion and Coulomb forces.

Intra-Tetrahedral Covalent Forces

Intra-tetrahedral forces are dominated by the four sp^3 hybrid orbitals protruding from the central silicon at mutual angles of 109.47°. Each orbital forms a strong covalent bond with an oxygen ion. The bond's strength is attested to by the small range of Si–O distances observed in tetrahedral silicates: from about 1.6 to 1.68 Å (Hazen and Finger 1978; Gibbs 1982). We chose a Morse potential to represent the Si–O covalent bond (Morse 1929):

$$V_r = D\{\exp[-2\beta(r-r_0)] - 2\exp[-\beta(r-r_0)]\}. \quad (1)$$

Here D is the depth of the potential well, r_0 is the position of the potential minimum, and β controls the sharpness of the well. Following previous workers (e.g. Price and Parker 1984) we assume $\beta = 2$.

We model the directionality of the Si–O bond by including a potential which depends on the angle between two hybrid orbitals (or, in practice, the angle between the

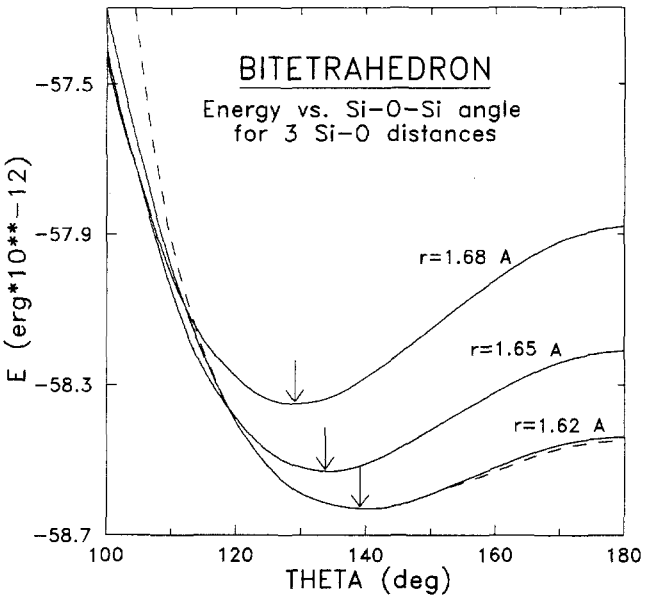

Fig. 2. Sections of constant r through the r vs. θ energy surface predicted by the ORM for the Si_2O_7 bitetrahedron. A comparison of the ORM without O–O repulsion (3 solid lines) with the complete ORM (dashed line) ($r = 1.62$ Å) shows that the inter-tetrahedral covalent force (Eq. 3) dominates inter-tetrahedral behavior

lines connecting two oxygen atoms to the central silicon atom):

$$V_\alpha = 0.5\, r_e^2\, k_\alpha (\alpha - \alpha_0)^2. \tag{2}$$

Here α_0 is the minimum energy O–Si–O angle of 109.47°, k_α is an O–Si–O angle-bending force constant and r_e is the equilibrium Si–O bond length.

Inter-Tetrahedral Covalent Forces

While the intra-tetrahedral forces serve primarily to keep the tetrahedra rigid, it is the inter-tetrahedral forces which control the compressional behavior of the model. Hence a careful consideration of the form of the inter-tetrahedral forces is crucial to the model's success. Some of the important qualitative features of these forces, as shown by the MO-derived Si–O distance (r) vs. Si–O–Si angle (θ) energy surface (Gibbs 1982), are: 1) the equilibrium θ decreases as r increases, 2) the angle bending force constant (f_θ) increases as θ decreases and 3) it is much easier to increase θ significantly than it is to decrease it.

While simple quadratic potentials in r and θ can match the surface only near the minimum (Lasaga and Gibbs 1987), we find that the potential:

$$V_L = 0.5\, k_L (L - L_0)^2, \tag{3}$$

together with the Morse potential, reproduce these qualitative features of the r vs. θ surface quite well. Here, L is the separation of Si atoms in corner sharing tetrahedra, and k_L and L_0 are the L stretching force constant (f_L) and the equilibrium value of L, respectively. Sections through the r vs. θ energy surface produced by the present model are shown in Figure 2. V_L is non-zero only between Si atoms of corner sharing tetrahedra, hence it is a three body force. It may be regarded as a Si–O–Si angle-bending force with a dependence on Si–O distance implicitly included.

Other Forces

The inclusion of O–O repulsion in the model is problematic, since its effect is difficult to separate from the Si–O–Si angle-bending force. That is, adding O–O repulsion or increasing the strength of the Si–O–Si force have similar effects on the properties of the Si_2O_7 molecule. Therefore, to help identify the simplest model which is consistent with the data we first consider a model without O–O repulsion that is constrained solely by the properties of the Si_2O_7 molecule. After pointing out its shortcomings, we add O–O repulsion by including the zero pressure equation of state parameters of quartz as constraints. We assume that the O–O repulsive potential is given by:

$$V_{OO} = A \exp(-r/b) \tag{4}$$

where A and b have units of energy and length, respectively.

We also tested the effects of Coulomb forces. Although splitting between longitudinal and transverse optic vibrations (Striefler and Barsch 1975) provides direct evidence for the existence of ionic charge in quartz, the magnitudes of the charges are not experimentally constrained. Following Pauling (1980), we have assumed that the charges on Si and O are 1 and $-1/2$, respectively.

The program WMIN (Busing 1981) was used to calculate the structure and density predicted by the model as functions of pressure. Given a potential model, WMIN minimizes the enthalpy of a crystal structure by adjusting its structural parameters. It is a static simulation technique, i.e. it does not account for the effects of temperature or zero point vibration. To compare the results of WMIN to experimental data, a Debye model thermal correction is applied to the static results.

Thermal Corrections

The total pressure is given by:

$$P(V, T) = P_{st}(V) + P_z(V) + P_{th}(V, T) \tag{5}$$

where P_{st} is the static pressure, P_z is the pressure due to zero point vibrations and P_{th} is the thermal pressure. P_z and P_{th} are significant, since their sum is on the order of 1 GPa for quartz and coesite. Quantitatively accurate values require the calculation of the phonon spectrum. Given the approximate nature of the potential, it is sufficient for our purposes to use the Debye approximation:

$$P_z(V) = (9/8)\, n k_b\, \gamma(V)\, \theta(V)/V \tag{6}$$

$$P_{th}(V) = [9 n k_b\, \gamma(V)/V]\, x_D^3 \int_0^{x_D} x^3\, dx/(1 - e^x) \tag{7}$$

where n is the number of atoms in the unit cell, k_b is Boltzmann's constant, γ is the thermal Grüneisen parameter, V is the unit cell volume and x_D is the ratio of the temperature to the thermal Debye temperature, θ (cf. Born and Huang 1954). The volume dependence of γ is approximated by (Anderson 1968):

$$\gamma(V) = \gamma_0 (V/V_0)^q \tag{8}$$

where γ_0 is the value of γ at V_0, and the parameter q was varied from 0 to 2, the range appropriate for most crystalline materials (Wallace 1972; Anderson 1974; Boehler 1982). The volume dependence of θ is then given by (Born and Huang 1954):

$$\theta(V)=\theta_0 \exp[(\gamma_0-\gamma)/q] \quad (9)$$

where θ_0 is the value of θ at V_0.

Values of θ_0 for quartz and coesite were taken from Kieffer (1979), which differ by less than 1 percent from the high temperature (350 K–700 K) average values calculated by Watanabe (1982). This is expected since θ is not very sensitive to temperature at room temperature (Kieffer 1979). γ_0 for quartz is reported by Boehler et al. (1979) and Boehler (1982). We adopt the former authors' value since they used a fluid pressure medium rather than the nonhydrostatic solid pressure medium of the latter author. The adopted value, $\gamma_0(\text{quartz})=0.675$, is consistent with the high temperature (350 K–700 K) average $\gamma(0.68\pm0.07)$ calculated by Watanabe (1982) since γ is nearly independent of temperature (Anderson 1968; Boehler 1982). γ_0 for coesite was calculated from the following identity:

$$\gamma=K_s \alpha v/C_p$$

where K_s is the adiabatic zero pressure bulk modulus, α is the thermal expansivity, v is the molar volume and C_p is the molar heat capacity at constant pressure. We take K_s from the 'preferred model' of Weidner and Carlton (1977), α from Skinner (1962), v from Levien and Prewitt (1981), and C_p from Robie et al. (1978). The value thus calculated:

$$\gamma_0(\text{coesite})=0.37\pm0.04$$

is equivalent to the high temperature average (350 K–700 K) calculated by Watanabe (1982) (0.352 ± 0.001). The quoted uncertainty in γ is an estimate and is due mostly to estimated uncertainties in α.

No additional thermal correction is applied for the effects that temperature may have on the crystal structure independent of volume changes. The implicit assumption is that the crystal structure is a unique function of the volume from 0 K to 300 K. To test this assumption, Table 1 compares the low temperature quartz structure observed by Lager et al. (1982) with that expected by interpolating the data of Levien et al. (1980) to the observed low temperature volume. The table shows that our assumption is valid for L, but not for r and σ. Thus, r and σ should be compared directly to low temperature data while our predicted L can be accurately compared to 300 K data. The last column of the table shows that changes in σ and L with pressure can be accurately compared to 300 K data. The table suggests that the change in r with pressure cannot be compared to 300 K data. However, the maximum change in r over the relevant temperature or pressure interval is only 0.2 percent of its absolute value. It is only this qualitative feature of rigidity which is relevant for bulk compression. The table also shows that L is the best measure of inter-tetrahedral distance for our purposes (rather than θ) since it is affected much less by temperature.

The above analysis cannot be repeated quantitatively for coesite since the structural differences between 15 K and 292 K measured by Smyth et al. (1987) are less than those between the two relevant sets of room temperature data (Smyth et al. 1987; Levien and Prewitt 1981). In fact, the structural differences between 15 K and 292 K were smaller than experimental error for r and σ and for 3 of the 5 Si–Si distances in the coesite structure. Therefore, for consistency, we compare our calculated coesite structures to the 300 K data of Levien and Prewitt (1981) at zero pressure and higher pressures.

Table 1. Temperature effects on the structure of quartz compared with temperature effects minus the attendant volume effects (purely thermal effects) and with pressure effects (over the experimental pressure range). Data are from Lager et al. (1982). High pressure data are from Levien et al. (1980)

	$T=296$ K	13 K obs.	13 K calc.[a]	$\frac{dT}{dT+dV}$[b]	$\frac{dT}{dP}$[c]
L(Å)	3.0577 (1)[d]	3.0530 (1)	3.0522	17%	0.8%
σ (deg)	0.84	0.92	0.88	50%	2%
r (Å)	1.610 (1)	1.613 (1)	1.610	100%	71%
θ (deg)	143.45 (6)	142.41 (6)	142.91	48%	5%

[a] 13 K calc. $\equiv X(296\text{ K})+dX/dV[V(13\text{ K})-V(296\text{ K})]$

[b] $\frac{dT}{dT+dV}\equiv\left|\frac{X(13\text{ K calc.})-X(13\text{ K obs.})}{X(296\text{ K})-X(13\text{ K obs.})}\right|$

[c] $\frac{dT}{dP}\equiv\left|\frac{X(13\text{ K calc.})-X(13\text{ K obs.})}{X(P=6.14\text{ GPa})-X(P=0\text{ GPa})}\right|$

where X is the relevant structural quantity in Quartz:
L: Si–Si distance
σ: standard deviation of O–Si–O angles
r: average tetrahedral Si–O distance
θ: Si–O–Si angle
V: is the unit cell volume, and dX/dV is the change in the structural quantity w.r.t V as calculated from the 300 K data of Levien et al. (1980)

[d] Estimated standard deviation of the last digit as reported

To compare the calculated transition pressure between quartz and coesite with experimental results, a thermal correction is applied to the calculated free energies of the two phases:

$$G(T,P)=G(0,P)-\int_0^T S\,dT \quad (10)$$

where $G(T,P)$ is the Gibbs free energy as a function of temperature and pressure, and S is the entropy calculated by integrating the Debye heat capacity over temperature. $G(0,P)$ is the zero temperature free energy:

$$G(0,P)=E_{st}+E_z+(P_{st}+P_z)V \quad (11)$$

where E_{st} is the static internal energy, E_z is the zero point vibration energy, and V is the volume at zero temperature.

Uncertainties in the thermal correction parameters (especially q) lead to uncertainties in calculated 300 K pressures of $\approx$0.1 GPa and in the free energies of $\approx$0.3 percent. The combined uncertainties in pressure and free energy lead to uncertainties in calculated transition pressures of 1–2 GPa.

Constraints

Model parameters and the procedures used to constrain them are summarized in Table 2. Although the parameters satisfy all the constraints simultaneously, each can be identified with an analogous physical quantity which constrains it most strongly. The parameters are uniquely determined for each model since their number is equal to the number of constraints and each constraint is matched within its reported experimental uncertainty. The parameters depend

Table 2. Values of parameters for the ORM (Oxygen Repulsion Model), CM (Charge Model) and SRM (Short Range Model) and the physical quantities used to constrain them. Listed with each parameter is the physical quantity which constraints it most strongly

	SRM	ORM	CM	Constraints
D(E)[a]	6.71	7.33	7.05	$f_r = 66\,\mathrm{E/L^2}$ [b]
$\beta(\mathrm{L}^{-1})$	2	2	2	assumed
r_0(L)	1.61900	1.60429	1.62758	$r_e = 1.619\,\mathrm{L}$ [b]
$k_\alpha(\mathrm{E/L^2})$	4.74	2.97	1.19	$f_\alpha = 4.74\,\mathrm{E/L^2}$ [c]
α_0(deg)	109.47	109.47	109.47	assumed
$k_L(\mathrm{E/L^2})$	14.00	8.76	4.48	$f_L = 14\,\mathrm{E/L^2}$ [b,e]
				$K_0 = 37.1$ GPa [d,e]
L_0 (L)	3.03294	3.03250	2.89340	$L_e = 3.03294\,\mathrm{L}$ [b]
A (E)	0	7.5E6	2.8E4	$\rho_0 = 2.646$ g/cc [d]
b (L)	0	0.14	0.22	$K_0' = 6.3$ [d]

[a] E and L refer to energy and length units respectively: E $= 10^{-12}$ erg; L = 1 Angstrom
[b] $H_6Si_2O_7$ MO calculation (O'Keeffe and McMillan 1986)
[c] H_4SiO_4 MO calculation (Hess et al. 1986)
[d] Zero Pressure EOS parameters for Quartz (Levien et al. 1980)
[e] f_L constrains the SRM while K_0 constrains the ORM and CM

on which forces are included and so are different for the three models.

As mentioned above, we first constrain and test a model which neglects O−O repulsion. The parameters of this *Short Range Model* (SRM) are constrained only by the structure and force constants of the $H_6Si_2O_7$ molecule determined by MO calculations (O'Keeffe and McMillan 1986).

Birch-Murnaghan EOS parameters (Birch 1978) for this and other models are summarized in Table 3. The SRM predicts a K_0' much smaller than experiment. Also, the zero pressure density and the zero pressure bulk modulus are overestimated.

The large bulk modulus of the SRM is due in part to the inaccuracy of the force constant f_L used as a constraint. f_L is overestimated by the MO calculations but the magnitude of the error is not known (O'Keeffe and McMillan 1986). Because of this uncertainty, we replace f_L by the closely related zero pressure bulk modulus K_0 of quartz (O'Keeffe et al. 1980). With this new constraint, the SRM is still unable to give accurate values of the zero pressure density and pressure derivative of the bulk modulus, K_0'.

Inclusion of O−O repulsion results in a significant improvement over the SRM model. To accommodate the two additional parameters in Equation 4, we add the zero pressure density and K_0' of quartz to the constraints. We call this model the *Oxygen Repulsion Model* (ORM). Addition of Coulomb interactions to the ORM results in the *Charge Model* (CM), which yields slight improvements in the predicted structures, but predicts a less accurate equation of state for coesite. To avoid the use of additional solid state data, no attempt was made to invert for optimal ionic charges. Instead, we followed Pauling's (1980) recommendation of +1 for Si and $-{}^1/_2$ for O.

Results

The Si−O bond strengths predicted by the models ($\approx 7 \times 10^{-12}$ erg for the SRM and ORM and $\approx 14 \times 10^{-12}$ erg for the CM) span the range of experimental estimates ($7\text{–}13 \times 10^{-12}$ erg; cf. Erikson and Hostetler 1987). This gives us confidence that the Morse potential is an appropriate model for the Si−O bond since the D parameter (Eq. 1) is found independently of bond strength data. Figure 1 shows that the exact strength of the Si−O bond is not important for modeling the compression of crystalline phases since rigid tetrahedra (infinite bond strength) are nearly consistent with the data. However, accurate prediction of the Si−O bond strength may be important in the liquid phase where the breaking of Si−O bonds could contribute significantly to compression.

In agreement with the arguments summarized in Figure 1, the inter-tetrahedral force is much weaker than the intra-tetrahedral forces. The barrier to linearity of the Si−O−Si angle ($\theta = 180°$) at the equilibrium r, is only 3 percent of the Si−O bond energy (see Figure 2). Because it is so weak, and because approximately correct values of

Table 3. Comparison of experimental Birch-Murnaghan EOS parameters for quartz and coesite with results of the ORM (Oxygen Repulsion Model), CM (Charge Model), SRM (Short Range Model) and previous models of SiO_2. Experimental values are from Levien et al. (1980) and Levien and Prewitt (1981)

	Quartz				Coesite		
	θ (deg)	ρ_0 (g/cc)	K_0 (GPa)	K_0'	ρ_0 (g/cc)	K_0 (GPa)	K_0'
Data	143.7	2.646	37.1	6.3	2.919	96	8.4
ORM	142.0	2.646*	37.2*	6.3*	2.898	78	3.2
CM	143.3	2.645*	37.1*	6.5*	2.886	84	4.6
SRM	140.6	2.682	58.4	0.7	2.936	95	−3.0
LG[a] covalent	144.0	2.685	39.4	−9.3			
LG[a] fractional ionic	164.6	2.320	11.9				
Mitra[b] fractional ionic			195			213	
⟨Fully ionic⟩[c]			200–784			314–860	

* Quantity used as a constraint

[a] Lasaga and Gibbs (1987)
[b] Mitra (1982)
[c] Range of 5 fully ionic models including: Woodcock et al. (1976), Lasaga and Gibbs (1987), Soules (1979), Matsui et al. (1982) and Hosteler (1982) from the results of Erikson and Hostetler (1987)

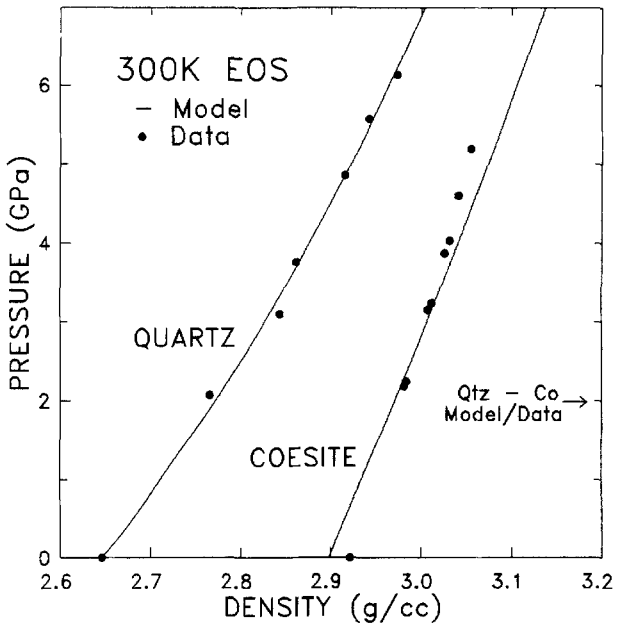

Fig. 3. Equations of state for quartz and coesite predicted by the ORM compared to the experimental data of Levien et al. (1980) and Levien and Prewitt (1981)

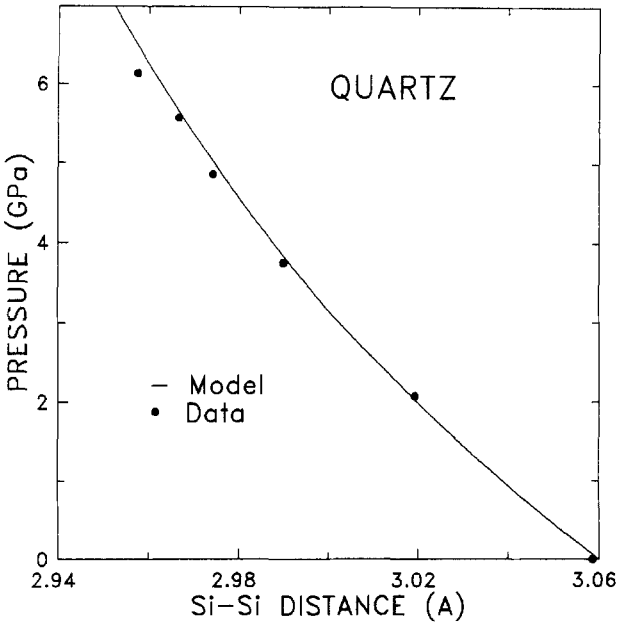

Fig. 4. The Si–Si distance in quartz as a function of pressure for the ORM compared with the data of Levien et al. (1980)

θ may be obtained with ionic pair potentials (e.g., Erikson and Hostetler 1987), we next examine the effect of eliminating this force from the model.

Without the inter-tetrahedral force, the model predicts β-quartz rather than α-quartz as the stable phase at $P=0$ and $T=300$ K. β-quartz is a special high symmetry case of α-quartz, stable above 848 K (Mirwald and Massonne 1980; but see Dolino et al. 1984) which contains the maximum value of $\theta(\theta\approx 160°$ compared with $\theta\approx 144°$ for α-quartz at zero pressure) allowed by the quartz structure (Grimm and Dorner 1975). The same result is obtained if we eliminate only its attractive part (V_L defined as zero for $L>L_0$), reducing it to a central repulsive force similar to those used in simple ionic models. Results published so far for simple ionic models (Lasaga and Gibbs 1987) show that these models also predict β-quartz as the stable zero pressure phase. This indicates that the weak angle bending covalent potential (Eq. 3) associated with the bridging oxygen must be included in accurate structural studies of silica.

Equation of State and Transition Pressure

The calculated EOS of quartz and coesite for the ORM are compared with experiment in Figure 3. Experimental data are from Levien et al. (1980) and Levien and Prewitt (1981). The calculated density of quartz agrees with experiment up to 6 GPa. Since Quartz EOS parameters were used as constraints, the coesite EOS provides a better test of the model. The model underestimates the zero pressure density of coesite by 0.8 percent. Also, the calculated coesite EOS is a little softer than the experimental one. Nevertheless, the calculated densities are within 1 percent of experiment up to 6 GPa, even though no coesite data was used to constrain the model.

The calculated quartz-coesite transition pressure is 1.7 GPa with an error of approximately 1 GPa due to uncertainties in the thermal corrections. This result agrees with the 2 ± 0.2 GPa transition pressure observed experimentally (Liu and Bassett 1986).

The CM underestimates the zero pressure density of coesite more severely than the ORM (1.1 %). However, K_0 and K_0' are in slightly better agreement with experiment. The quartz-coesite transition pressure is 4.5 ± 2 GPa for the CM.

Structure and Compression Mechanisms

Upon compression the Si–O–Si angle in tetrahedral SiO_2 decreases while the SiO_4 tetrahedra remain nearly rigid. For a model of SiO_2 to be successful it must reproduce these most important qualitative features of compression in SiO_2. The change in calculated Si–Si distances with pressure is compared with experiment (Levien et al. 1980) in Figures 4 (quartz) and 5 (coesite). In quartz, the calculated Si–Si distance agrees with experiment up to 6 GPa. Coesite provides a more stringent test of the model, since no coesite data were used as constraints and since coesite has a more complex, lower symmetry structure than quartz. In coesite, the agreement with experiment (Levien and Prewitt 1981) is less quantitative than in quartz but the important trends are reproduced. The order of the Si–Si distances from smallest to largest is reproduced within the calculated stability field of coesite. Also reproduced by the model is the counter-intuitive result that the smaller Si–Si distances decrease more with pressure than the larger ones.

For quartz and coesite the calculated tetrahedra are relatively undeformable compared to the Si–O–Si angle, in agreement with experiment (see Table 4). Further, as is observed, the calculated Si–O bond length decreases with pressure and the deviation of the O–Si–O angles from the ideal value of 109.47° increases with pressure. However, the calculated rigidity of the tetrahedra is somewhat larger than that observed. The standard deviation of the O–Si–O angles (σ) and the increase in σ with pressure is underesti-

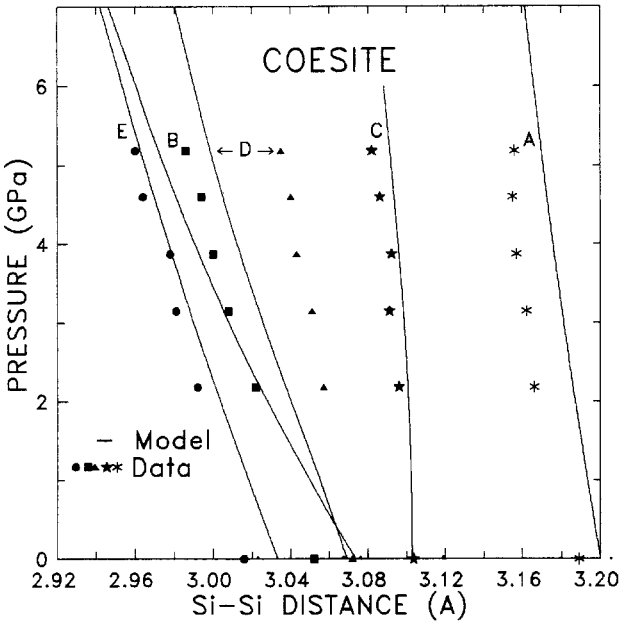

Fig. 5. The Si–Si distances in coesite as a function of pressure for the ORM and experiment. The labels *A–E* are those of Levien and Prewitt (1981)

Table 4. Tetrahedral geometries and their changes with pressure for the ORM and experiment. Zero pressure data for quartz is from Lager et al. (1982). Data for changes in r and σ with pressure is from Levien et al. (1981). Coesite data is from Levien and Prewitt (1981)

	r(Å)	σ(deg)[a]	dr (Å)	$d\sigma$ (deg)[b]
Quartz				
Data	1.613 (1)[c]	0.92 (5)	−0.004 (2)	1.4 (2)
ORM	1.618	0.11	−0.002	0.7
Coesite				
Data 1[d]	1.6092 (6)	0.90 (6)	−0.006 (2)	0.4 (3)
ORM 1	1.6121	0.25	−0.007	0.9
Data 2	1.6118 (6)	0.42 (7)	−0.007 (3)	0.3 (3)
ORM 2	1.6158	0.28	−0.004	0.2

[a] Low temperature experimental data are shown for r (average tetrahedral Si–O distance) and σ (standard deviation of O–Si–O angles)

[b] 300 K data are shown for dr and $d\sigma$ (change in r and σ, respectively over the experimental pressure range)

[c] Estimated standard deviation of the last digit reported

[d] 1 and 2 following Data and ORM refer to the tetrahedra containing Silicon 1 and Silicon 2 in the coesite structure as labelled by Levien and Prewitt (1981)

mated by the model. Also, the calculated Si–O bond length is too large and the change in Si–O bond length with pressure too small.

While the change in Si–Si distances with pressure is similar for the ORM and CM, the latter predicts smaller and more deformable tetrahedra (in quartz: $r=1.612$ Å, $\sigma=0.41$ deg at $P=0$; −0.005 Å change in r, 1.2 deg change in σ up to 6 GPa), in better agreement with experiment. However, we do not regard this as a significant advantage of the CM over the ORM since the compressional behavior of tetrahedra, as long as they remain nearly rigid, is unimportant for the compression of SiO_2 framework structures (see Figure 1).

Discussion and Conclusions

We have constructed two covalent potential models of tetrahedral phases of SiO_2 that are independent of solid state structural data. One of the models (CM) includes Coulomb interactions, while the other (ORM) does not. By design, the models combine simplicity with essential qualitative features of the physics of SiO_2 bonding, including the dichotomy between strong intra- and weak inter-tetrahedral forces, and a form of inter-tetrahedral forces suggested by molecular orbital calculations. The models reproduce the structure, compressibility and compression mechanisms of quartz and coesite, and the transition pressure between them, with good accuracy. Therefore, these models should prove particularly suitable for efficient and accurate simulations of not only crystalline phases of SiO_2 but also liquids and glasses.

The model that includes Coulomb forces (CM) produces tetrahedral geometries and a coesite compressibility that are in slightly better agreement with experiment. The predicted quartz-coesite transition pressure and zero pressure density of coesite, are less accurate than those derived from the ORM. However, given the approximate nature of the thermal corrections, it is not clear that the small differences in structural detail are very significant. Therefore, since the Coulomb energy term is not clearly necessary, the simpler ORM is to be preferred.

Upon compression, it is likely that the structure of liquid SiO_2, by analogy with the solid phases of SiO_2, undergoes a change from larger (5–8 membered) to smaller (3–5 membered) rings of tetrahedra (Hemley et al. 1986). The transformation from quartz (predominantly 6-membered rings) to coesite (predominantly 4-membered rings) is an example of such a transition. The ORM accurately represents the equations of state of both phases and the transition between them. This gives us confidence that the model will accurately predict the structure of liquid SiO_2 at moderate pressures (i.e., pressures below those where octahedral coordination may become important).

Acknowledgments. We thank Q. Williams, A. Agnon and G.V. Gibbs for helpful comments on the manuscript. This research was supported by NSF grant EAR-8707283 and the Institute of Geophysics and Planetary Physics at the Lawrence Livermore National Laboratory, University of California.

References

Akimoto S, Yagi Y, Inoue K (1977) High temperature-pressure phase boundaries in silicate systems using in situ X-ray diffraction. In: Akimoto S, Manghnani MH (eds) High pressure research in geophysics. Center for Academic Publications, Tokyo, Japan

Anderson OL (1968) Some results on the volume dependence of the Grüneisen parameter γ. J Geophys Res 73:5187–5194

Anderson OL (1974) The determination of the volume dependence of the Grüneisen parameter. J Geophys Res 79:1153–1155

Bass JD (1987) Mineral and melt physics. Rev Geophys 25:1215–1276

Birch F (1978) Finite strain isotherms and velocities for single-crystal and polycrystalline NaCl at high pressures and 300° K. J Geophys Res 83:1257–1268

Boehler R (1982) Adiabats of quartz, coesite, olivine and magne-

sium oxide to 50 kbar and 1000 K, and the adiabatic gradient in the Earth's mantle. J Geophys Res 87:5501–5506
Boehler R, Skoropanov A, O'Mara D, Kennedy GC (1979) Grüneisen parameter of quartz, quartzite and fluorite. J Geophys Res 84:3527–3531
Born M, Huang K (1954) Dynamical theory of crystal lattices. Oxford University Press, pp 420
Busing WR (1981) WMIN. A computer program to model molecules and crystals in terms of potential energy functions. Oak Ridge National Laboratory, Oak Ridge
Dolino G, Bachheimer JP, Berge B, Zeyen CME, Van Tendeloo G, Van Landuyt J, Amelinckx S (1984) Incommensurate phase of quartz: III. Study of the coexistence state between the incommensurate and the α-phases by neutron scattering and electron microscopy. J Physique 45:901–912
Erikson RL, Hosteler CJ (1987) Application of empirical ionic models to SiO_2 liquid: potential model approximations and integration of SiO_2 polymorph data. Geochim Cosmochim Acta 51:1209–1218
Gibbs GV (1982) Molecules as models for bonding in silicates. Am Mineral 67:421–450
Grimm H, Dorner B (1975) On the mechanism of the $\alpha-\beta$ quartz phase transformation of quartz. J Phys Chem Solids 36:407–413
Hazen RM, Finger LW (1978) Crystal chemistry of silicon-oxygen bonds at high pressure: implications for the Earth's mantle mineralogy. Science, 201:1122–1123
Hemley RJ, Mao HK, Bell PM, Mysen BO (1986) Raman spectroscopy of SiO_2 glass at high pressure. Phys Rev Lett 57:747–750
Hess AC, McMillan PF, O'Keeffe M (1986) Force fields for SiF_4 and H_4SiO_4: ab initio molecular orbital calculations. J Phys Chem 90:5661–5665
Hostetler CJ (1982) Equilibrium properties of some silicate materials: a theoretical study. Ph D dissertation, Univ. Arizona
Jeanloz R, Thompson AB (1983) Phase transitions and mantle discontinuities. Revs Geophys and Space Phys 21:51–74
Jorgensen JD (1978) Compression mechanisms in α-quartz structures – SiO_2 and GeO_2. J Appl Phys 49:5473–5478
Kieffer SW (1979) Thermodynamics and lattice vibrations of minerals: 3. lattice dynamics and an approximation for minerals with application to simple substances and framework silicates. Revs Geophys and Space Phys 17:35–59
Lager GA, Jorgensen JD, Rotella FJ (1982) Crystal structure and thermal expansion of α-quartz SiO_2 at low temperatures. J Appl Phys 53:6751–6756
Lasaga AC, Gibbs GV (1987) Applications of quantum mechanical potential surfaces to mineral physics calculations. Phys Chem Minerals 14:107–117
Levien L, Prewitt CT, Weidner DJ (1980) Structure and elastic properties of quartz at pressure. Am Mineral 65:920–930
Levien L, Prewitt CT (1981) High-pressure crystal structure and compressibility of coesite. Am Mineral 66:324–333
Liu L, Bassett WA (1986) Elements, oxides, silicates; high pressure phases with implications for the Earth's interior. Oxford University Press, pp 250
Matsui Y, Kawamura K, Syono Y (1982) Molecular dynamics calculations applied to silicate systems: molten and vitreous $MgSiO_3$ and Mg_2SiO_4 under low and high pressures. Adv Earth Planet Sci 12:511–524
Mirwald PW, Massonne HF (1980) The low-high quartz and quartz-coesite transition to 40 kbar between 600-degrees-C and 1600-degrees-C and some reconnaissance data on the effect of $NaAlO_2$ component on the low quartz-coesite transition. J Geophys Res 85:6983–6990
Mitra SK (1982) Molecular dynamics simulation of silicon dioxide glass. Phil Mag B 45:529–548
Morse PM (1929) Diatomic molecules according to the wave mechanics. II. Vibrational levels. Phys Rev 43:57–67
O'Keeffe M, Newton MD, Gibbs GV (1980) Ab initio calculation of interatomic force constants in $H_6Si_2O_7$ and the bulk modulus of α quartz and α cristobalite. Phys Chem Minerals 6:305–312
O'Keeffe M, McMillan PF (1986) The Si–O–Si force field: ab initio MO calculations. J Phys Chem 90:541–542
Pauling L (1980) The nature of silicon-oxygen bonds. Am Mineral 65:321–323
Price GD, Parker SC (1984) Computer simulations of the structural and physical properties of the Olivine and Spinel polymorphs of Mg_2SiO_4. Phys Chem Minerals 10:209–216
Robie RA, Hemingway BS, Fisher JR (1978) Thermodynamic properties of minerals and related substances at 298.15 K and one bar (10^5 pascals) pressure and at high temperatures. US Geol Surv Bull 1452
Sanders MJ, Leslie M, Catlow CRA (1984) Interatomic potentials for SiO_2. J Chem Soc, Chem Commun 1271–1274
Skinner BJ (1962) Thermal expansion of ten minerals. US Geol Surv Prof Paper 450D:109–112
Smyth JR, Smith JV, Artioli G, Kvick A (1987) Crystal structure of coesite, a high-pressure form of SiO_2 at 15 and 298 K from single-crystal neutron and x-ray diffraction data: test of bonding models. J Phys Chem 91:988–992
Soules TF (1979) A molecular dynamic calculation of the structure of sodium silicate glasses. J Chem Phys 71:4570–4578
Striefler ME, Barsch GR (1975) Lattice Dynamics of α quartz. Phys Rev B 12:4553–4566
Wallace D (1972) Thermodynamics of crystals. J Wiley and Sons, Inc., New York, p 357
Watanabe H (1982) Thermochemical properties of synthetic high-pressure compounds relevant to the Earth's mantle. In: Akimoto S, Manghnani MH (eds) High pressure research in geophysics. Center for Academic Publications, Tokyo, Japan
Weidner DJ, Carleton HR (1977) Elasticity of coesite. J Geophys Res 82:1334–1346
Williams Q, Jeanloz R (1988) Spectroscopic evidence for pressure-induced coordination changes in silicate glasses and melts. Science 239:902–905
Woodcock LV, Angell CA, Cheeseman P (1976) Molecular dynamics studies of the vitreous state: simple ionic systems and silica. J Chem Phys 65:1565–1577

Received February 9, 1988